JOURNAL OF VIROLOGY, Mar. 1997, p. 2100–2106 Vol. 71, No. 3
0022-538X/97/$04.00+0

Reovirus Infection and Tissue Injury in the Mouse Central Nervous System Are Associated with Apoptosis

STEPHANIE M. OBERHAUS,[1] RODERIC L. SMITH,[1,2] GERALD H. CLAYTON,[1] TERENCE S. DERMODY,[3,4,5] AND KENNETH L. TYLER[1,6,7]*

Departments of Neurology,[1] Pediatrics,[2] and Microbiology, Immunology, and Medicine,[6] University of Colorado Health Sciences Center, Denver, Colorado 80262; Neurology Service, Denver Veterans Affairs Medical Center, Denver, Colorado 80220[7]; and Departments of Pediatrics[3] and Microbiology and Immunology,[4] and the Elizabeth B. Lamb Center for Pediatric Research,[5] School of Medicine, Vanderbilt University, Nashville, Tennessee 37232

Received 21 October 1996/Accepted 13 December 1996

Reovirus serotype 3 strains infect neurons within specific regions of the neonatal mouse brain and produce a lethal meningoencephalitis. Viral replication and pathology colocalize and have a predilection for the cortex, hippocampus, and thalamus. We have shown previously that infection of cultured fibroblasts and epithelial cells with reovirus type 3 Dearing (T3D) and other type 3 reovirus strains results in apoptotic cell death, suggesting that apoptosis is a mechanism of cell death in vivo. We now report that T3D induces apoptosis in infected mouse brain tissue. To determine whether reovirus induces apoptosis in neural tissues, newborn mice were inoculated intracerebrally with T3D, and at various times after inoculation, brain tissue was assayed for viral antigen by immunostaining and apoptosis was identified by DNA oligonucleosomal laddering and in situ terminal deoxynucleotidyl transferase-mediated dUTP nick end labeling. Cells were also stained with cresyl violet to detect morphological changes characteristic of apoptosis, including chromatin condensation and cell shrinkage. DNA laddering was detected in T3D- but not in mock-infected brain tissue. Apoptotic cells were restricted to the same regions of the brain in which infected cells and tissue damage were observed. These findings suggest that virus-induced apoptosis is a mechanism of cell death, tissue injury, and mortality in reovirus-infected mice. The correlation between apoptosis and pathogenesis in vivo identifies apoptosis as a potential target for molecular and pharmacological strategies designed to curtail or prevent diseases resulting from induction of this cell death pathway.

Apoptosis is a distinct mechanism of cell death which can be induced by a variety of internal and external stimuli (10). This process serves primarily to eliminate cells during normal development and immune cell selection as well as cells that have sustained genetic damage. Apoptotic cells are characterized by specific changes in cell morphology, including cytoplasmic shrinkage, chromatin condensation, and eventually fission into multiple, membrane-bound apoptotic bodies (reviewed in reference 27). DNA isolated from apoptotic cells is often fragmented into oligonucleosomes (fragment length multiples of 180 to 200 bp), resulting from cleavages at internucleosomal regions by an endogenous endonuclease. Since apoptotic cells remain membrane bound and are generally phagocytosed by resident macrophages, apoptosis is seldom associated with an inflammatory response. In contrast, necrotic cell death, which occurs in response to acute cellular damage, is characterized by cellular alterations that differ from those characteristic of apoptosis, including cell swelling, random degradation of chromatin, and eventually cell lysis (16). The release of intracellular constituents as a result of membrane breakdown usually elicits an inflammatory response.

Numerous viruses have been shown to induce apoptosis in cultured cells (24, 28), and a correlation between infection and induction of apoptosis in vivo has been demonstrated for a subset of these viruses, including influenza virus (18), measles virus (1), Sindbis virus (13), human immunodeficiency virus (HIV) (4, 23), Theiler's murine encephalomyelitis virus (29), and La Crosse virus (22). However, the role of apoptosis in viral pathogenesis in vivo has not been clearly established. For viral infections which lead to the death of nonrenewable cells, like neurons, an understanding of the mechanism of cell death is especially critical.

Reovirus infection of neonatal mice has served as a useful model system for the study of many aspects of viral pathogenesis, including spread within the host, cell tropism, and virulence (reviewed in reference 31). Strain-specific differences in pathogenesis and the segmented nature of the reovirus genome have allowed identification of the functions of individual gene products at distinct stages of the virus-host interaction. The central nervous system (CNS) tropism and neurovirulence of reoviruses are determined by the viral S1 and M2 genes which encode outer capsid proteins involved in cell attachment and entry (8, 11, 14, 20, 36, 37). Reovirus strain T3 Dearing (T3D) primarily infects neurons within the cortex, thalamus, and hippocampus, and infected animals succumb to a lethal encephalitis. Pathological examination of brain tissue obtained from T3D-infected mice shows focal areas of neuronal destruction in the absence of a significant early inflammatory response (31).

We have shown previously that reovirus induces apoptosis in cultured fibroblasts (32, 33) and epithelial cells (25), and that this capacity is determined primarily by the S1 gene. In this study, we used strain T3D to determine whether reovirus induces apoptosis in the mouse CNS. In situ assays for apoptosis and viral antigens were used to determine whether apoptosis was associated with viral infection and pathology. Our results

* Corresponding author. Mailing address: Department of Neurology (B-182), University of Colorado Health Sciences Center, 4200 E. Ninth Ave., Denver, CO 80262. Phone: (303) 393-2874. Fax: (303) 393-4686. E-mail: tylerk@essex.uchsc.edu.

indicate that virus-induced apoptosis is an important component of reovirus-induced tissue injury in the CNS.

MATERIALS AND METHODS

Cells and virus. Mouse L929 fibroblasts (L cells) (ATCC CCL1) were passaged in spinner culture by adjusting the cell concentration daily to 5×10^5 cells/ml by dilution with Joklik's modified Eagle minimum essential medium supplemented to contain 5% heat-inactivated fetal bovine serum and 2 mM L-glutamine (Gibco/BRL). Reovirus strain T3D is a laboratory stock which was plaque purified and passaged in L cells to generate working stocks as previously described (30).

Animals. One-day-old Swiss Webster mice [Tac:(SW)fBR; Taconic, Germantown, N.Y.] received inoculations intracerebrally (i.c.) into the right hemisphere with a Hamilton syringe and a 30-gauge needle. The inoculum consisted of either gel saline (mock infection) (35) or 10^4 PFU of reovirus T3D in gel saline in a volume of 10 μl. Animals were euthanized at 1, 3, 6, and 8 days postinfection (dpi), and brain tissue was removed. For determining viral titer and detection of DNA laddering, brain tissue was divided into halves along the midcoronal line. One half was placed in gel saline and stored at −80°C for viral titration; the other half was placed in Tris-EDTA (TE) buffer (10 mM Tris [pH 8.0], 1 mM EDTA) at −20°C for extraction of DNA. For histopathologic staining, whole brains were fixed by immersion in 4% paraformaldehyde in 0.1 M phosphate buffer (pH 7.2) at 4°C for 2 to 4 days, dehydrated, cut in half along the midcoronal line, embedded in paraffin, and sectioned.

Mice were maintained in an American Association for the Accreditation of Laboratory Animal Care-approved facility in accordance with National Institutes of Health-Centers for Disease Control and Prevention animal biosafety level-2 practices. Protocols for animal experiments were approved by the Animal Studies Subcommittee of the Denver Veterans Administration Medical Center and the Animal Care and Use Committee of the University of Colorado Health Sciences Center.

Determination of viral titer. Brain tissue in gel saline was sonicated briefly with a microtip probe (Ultrasonic XL sonicator) at setting 3 to homogenize tissue. Serial 10-fold dilutions were made in gel saline prior to inoculation of L-cell monolayers in six-well plates (10^6 cells per well). Duplicate wells for each of three dilutions were inoculated, and plaque assays were performed as described previously (35). The growth curve was generated using SlideWrite Plus for Windows (Advanced Graphics Software, Inc. Carlsbad, Calif.), which utilizes the least-squares regression method.

Detection of oligonucleosomal laddering. Brain tissue was homogenized in 10 volumes of TE buffer with a microcentrifuge tube pestle. EDTA was added to a final concentration of 10 mM, and Triton X-100 was added to a final concentration of 0.5%. Samples were vortexed, and low-molecular-weight DNA was isolated by centrifugation at 13,000 × *g* for 10 min at room temperature. Supernatants, which contained low-molecular-weight DNA, were collected and incubated overnight at 37°C in the presence of 0.5% sodium dodecyl sulfate and 0.1 mg of proteinase K (Boehringer Mannheim) per ml. DNA was isolated by phenol-chloroform extraction and precipitation with 95% ethanol. Purified DNA (10 μg per lane) was resolved by electrophoresis in a 1.5% agarose gel, transferred to a nylon membrane, and visualized by hybridization with a ^{32}P-labeled, nick-translated L-cell genomic DNA probe, as described previously (33).

Detection of fragmented DNA in situ. Terminal deoxynucleotidyl transferase (TdT)-mediated dUTP-biotin nick end-labeling (TUNEL) was used to detect cells containing fragmented DNA in 10-μM sections from mock- and T3D-infected mouse brains (6). Tissue sections were deparaffinized, rehydrated, and digested with 5 μg of proteinase K (Boehringer Mannheim) per ml in 10 mM Tris (pH 7.5)–2 mM $CaCl_2$ for 30 min at 37°C. After two 5-min washes in phosphate-buffered saline (PBS), sections were incubated with 0.3% H_2O_2 in PBS for 15 min at room temperature to inactivate endogenous peroxidase. Sections were washed twice with water and rinsed once with TdT buffer (30 mM Tris [pH 7.2], 140 mM sodium cacodylate, and 1 mM cobalt chloride). Tissue sections were covered with 75 μl of the labeling mixture (50 nmol of biotin-16-dUTP [Boehringer Mannheim] per ml and 500 to 750 U of TdT [Bethesda Research Laboratories] per ml in TdT buffer [supplied with TdT]), and incubated under a coverslip in a humidified chamber for 1 h at 37°C. The reaction was terminated by washing the sections with 4× SSC (1× SSC is 0.15 M NaCl plus 0.015 M sodium citrate) for 15 min at room temperature. Sections were then rinsed with water and incubated with 2% bovine serum albumin (Sigma) for 10 min at room temperature. After two 5-min washes in PBS, sections were incubated with the avidin-biotin complex in PBS (Vectastain Elite-ABC kit; Vector Laboratories) for 1 h at room temperature. After three 10-min washes in PBS, sections were stained by incubating for 1 to 3 min with the chromagen 3,3′-diaminobenzidine (DAB) (DAB substrate kit; Vector), resulting in the appearance of a reddish brown precipitate in positively stained nuclei.

Detection of viral antigens. Reovirus antigens were detected by immunocytochemistry with a rabbit polyclonal anti-T3D antiserum (35). Sections were deparaffinized, rehydrated, digested with proteinase K to enhance antigenicity, and treated with H_2O_2 as described above for the TUNEL assay. Alternatively, slides which had been assayed by TUNEL were stained for reovirus antigens after washing off the mounting solution. Following several PBS washes, sections were incubated in a blocking solution (0.2% Triton X-100, 2% normal rabbit serum, and 1% bovine serum albumin in PBS) for at least 30 min at room temperature. Sections were incubated with a 1:200 dilution of the primary antibody in the blocking solution overnight at 4°C. After three 10-min washes with PBS, sections were incubated with either a 1:50 dilution of fluorescein isothiocyanate (FITC)- or a 1:200 dilution of biotin-conjugated goat anti-rabbit serum in blocking solution for 1 h at 37°C. After three 10-min washes with PBS, sections incubated with the FITC-conjugated secondary antiserum were mounted with Aqua-Poly/Mount and viewed by epifluorescence microscopy (Nikon Labophot-2) using a fluorescein filter (B-2A). Sections incubated with the biotinylated secondary antiserum were incubated with the avidin-biotin complex and stained with DAB, as described for the TUNEL assay.

Cresyl violet staining. Sections were deparaffinized, rehydrated, and then stained with 0.5% cresyl violet (2), mounted with DPX (Aldrich), and viewed by light microscopy. Cresyl violet is a nucleic acid stain which, like Hoechst and DAPI (4′,6-diamidino-2-phenylindole), facilitates identification of chromatin and other cellular morphological changes associated with apoptosis.

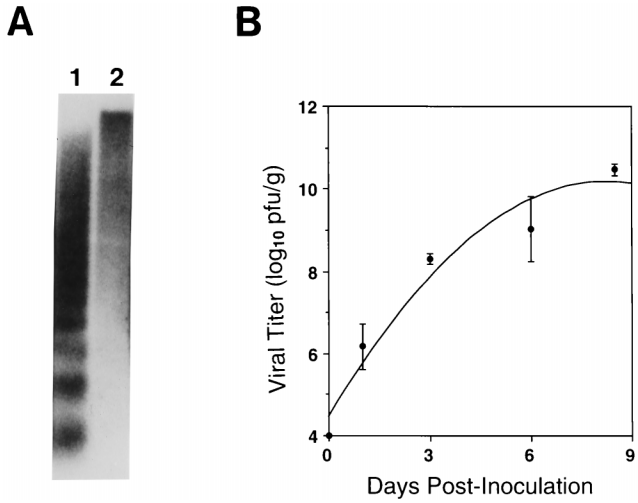

FIG. 1. (A) Autoradiograph of Southern blot hybridization of low-molecular-weight cellular DNA (10 μg/lane) extracted from T3D (lane 1)- or mock (lane 2)-infected mouse brains at 8 to 9 dpi. DNA was resolved by agarose gel electrophoresis, transferred to a nylon membrane, and hybridized with a ^{32}P-labeled, nick-translated, L-cell genomic DNA probe. (B) Growth of reovirus T3D in brain tissue. One-day-old Swiss Webster mice were inoculated i.c. with 10^4 PFU of T3D. Brain tissue was collected at 1, 3, 6, and 8 dpi. Virus titers in homogenized tissue were determined by plaque assay. The results are presented as the mean viral yields, with error bars indicating standard errors of the mean.

RESULTS

Reovirus induces apoptosis in infected mouse brain. To determine whether reovirus induces apoptosis in vivo, newborn mice were inoculated i.c. with strain T3D and brain tissue was collected 1, 3, 6, and 8 to 9 dpi. DNA was extracted from T3D- and mock-infected brains and analyzed by agarose gel electrophoresis and Southern blot hybridization. Fragmentation of cellular DNA into oligonucleosome-length ladders was observed in tissue samples prepared from T3D- but not mock-infected mice 8 to 9 dpi (Fig. 1A). Faint DNA laddering was detected at earlier time points but did not differ significantly in brain tissue taken from T3D- and mock-infected mice (data not shown). Laddering at these earlier time points most likely represents the normal apoptosis of cells which occurs during development of the mouse CNS (9, 21), since no laddering was detected at the later time point in mock-infected brain (8 to 9 dpi). These results indicate that reovirus T3D induces apoptosis in the mouse CNS. To determine whether induction of apoptosis correlated with viral growth, the viral titer in brain tissue was determined by plaque assay at 1, 3, 6, and 8 to 9 dpi. The titer increased at each time point and reached a peak of 10^9 PFU/g at 8 to 9 dpi, at which time the mice were moribund

(Fig. 1B). The growth curve was generated by using a second order polynomial equation with the formula $y = 5.02 + 1.11x - 0.059x^2$. The r value, which is an indication of how well the curve fits the data, is 0.98433 ($r^2 = 96.89$). These experiments demonstrate that detection of apoptosis by oligonucleosomal laddering coincided with maximal viral growth.

Viral replication, apoptosis, and tissue damage are restricted to distinct regions within the neonatal mouse brain. To determine whether apoptosis occurs within the same regions of the brain as reovirus replication and tissue injury, brain tissue sections from T3D-infected mice were either stained with cresyl violet to detect morphological evidence of apoptosis or double-stained for reovirus antigens and fragmented DNA to detect infected and apoptotic cells, respectively, at 3, 6, and 8 dpi. Reovirus antigens were detected by immunocytochemistry, and fragmented DNA was detected by the TUNEL assay. TUNEL results in labeling of the available 3′ OH ends of DNA frequently generated during apoptosis by endonuclease-mediated fragmentation. In addition, TUNEL facilitates identification of fragmented DNA which is also condensed, a prominent morphological feature of apoptosis. At 3 dpi, only a few TUNEL- and reovirus antigen-positive cells were detected in the thalamus, and pathologic injury was minimal. By 6 dpi, tissue damage within the cingulate gyrus and thalamus was extensive, and significant pathologic injury was observed in cortical layer V and throughout the hippocampus, including CA1 to CA3 and the dentate gyrus (Fig. 2A). Large numbers of antigen-positive and apoptotic cells were concentrated exclusively in these same regions, and there was no inflammation (Fig. 2B to G). At 8 dpi, there were increased numbers of reovirus antigen-positive and apoptotic cells in these same regions in conjunction with extensive tissue damage. Although we could often distinguish individual, labeled cells, this was not possible in many cases, making it impossible to accurately quantitate reovirus antigen-positive, TUNEL-positive, and doubly labeled cells. However, marked regional differences in the ratio of TUNEL- to reovirus antigen-positive signals could be observed. For example, it appeared that significantly more cells in the cingulate gyrus were TUNEL-positive than were antigen-positive as compared to those in the hippocampus, based on the relative amount of each signal present.

Many of the reovirus antigen-positive cells in these sections could be identified as neurons by morphological criteria, including prominent immunostaining of axonal and dendritic processes which contained large amounts of reovirus antigens (Fig. 2A, C, and E). Neither reovirus antigen-positive nor apoptotic cells were observed in white matter tracts, regions which do not contain neurons. These observations are consistent with the characteristic neuronal tropism of the T3D strain. Moreover, the early appearance in the mouse brain of reovirus antigen in the thalamic nuclei and the later appearance in the cingulate gyrus and cortical layer V suggest that the virus spread within the brain via neural pathways.

These data show that reovirus replication in distinct regions of infected mouse brain correlated with increasing numbers of apoptotic cells and tissue damage. Maximal numbers of reovirus antigen-positive cells and apoptotic cells and maximal levels of tissue damage were detected at 8 dpi, the same time point at which oligonucleosomal laddering was detected (Fig. 1A) and mice were moribund. The colocalization and parallel temporal development of viral antigen, apoptotic cells, and pathologic injury strongly suggest that apoptosis is a major mechanism of cell loss and tissue injury which ultimately leads to the death of T3D-infected mice.

Tissue injury and apoptosis in T3D-infected and mock-infected CNSs. To compare tissue damage and apoptosis in association with T3D and mock infections, sections obtained from T3D- and mock-infected mice at 3, 6, and 8 dpi were analyzed by (i) immunostaining for reovirus antigens, (ii) TUNEL, and (iii) cresyl violet staining. Figure 3 shows regions from the cingulate gyrus obtained from T3D- and mock-infected mice at 6 or 8 dpi. The findings for hippocampal and cortical regions were identical to the findings described for the cingulate gyrus (data not shown). At 3 dpi, TUNEL-positive cells were detected in brain sections obtained from both T3D- and mock-infected mice (data not shown). The majority of TUNEL-positive cells were observed in the cortical subplate which is involuting at this developmental stage. Rare TUNEL-positive cells were detected in brain tissue sections obtained from mock-infected mice at 6 or 8 dpi, and most of them were confined to the cortical subplate region (data not shown). None of the sections from mock-infected mice contained reovirus antigen-positive cells or evidence of tissue damage (Fig. 3B, D, and F). In contrast, sections from T3D-infected mice contained numerous reovirus antigen- and TUNEL-positive cells within the cingulate gyrus (Fig. 3A and C), hippocampus, and thalamus. Cresyl violet staining showed that there was also extensive tissue damage and altered cellular morphology consistent with apoptosis (cytoplasmic shrinkage and chromatin condensation) in these same regions (Fig. 3E).

Reovirus antigen and TUNEL rarely colocalize within the same cell. To determine whether apoptotic cells contained reovirus antigens, brain tissue sections from T3D-infected mice were assayed simultaneously for the presence of reovirus antigens by immunofluorescence and for apoptosis by TUNEL. In all infected regions, a mixture of doubly and singly labeled cells was observed (Fig. 4). Some cells contained both reovirus antigens and fragmented DNA, but it was often difficult to distinguish colabeling when single cells had appeared to shrink (Fig. 4A) and break into apoptotic bodies (Fig. 4B). Many cells were labeled for either reovirus antigens or fragmented DNA but not both (Fig. 4C and D). These results suggest that apoptosis in reovirus-infected regions of the brain occurs in both productively infected and uninfected cells.

DISCUSSION

Reovirus strain T3D infects neurons within the cortex, thalamus, and hippocampus of neonatal mice, resulting in neuronal cell death and lethal meningoencephalitis. In this study, we show a striking correlation between reovirus infection and induction of apoptosis which suggests reovirus-induced apoptosis is a major mechanism of cell death, tissue injury, and mortality in infected animals.

Our findings suggest that reovirus induces apoptosis of both reovirus antigen-positive and reovirus antigen-negative cells. However, the relative number of apparently infected and uninfected apoptotic cells was impossible to ascertain accurately. It was often difficult to associate TUNEL and/or reovirus antigen signals with individual cells because the cell bodies were not distinguishable (Fig. 4). There are several possible explanations for our observations. Many TUNEL-positive, reovirus antigen-negative cells had undergone extensive cytoplasmic shrinkage, which may have precluded the detection of antigen. Additionally, proteolysis of cytoplasmic proteins, which occurs during apoptosis, may have altered or degraded antigenic sites beyond recognition (15). Since reovirus replicates exclusively in the cytoplasm, these events could result in an underestimation of the number of reovirus antigen-positive cells undergoing apoptosis. TUNEL-positive, reovirus antigen-negative cells could also result from the apoptotic death of an uninfected neuron which has lost trophic support from a connecting cell

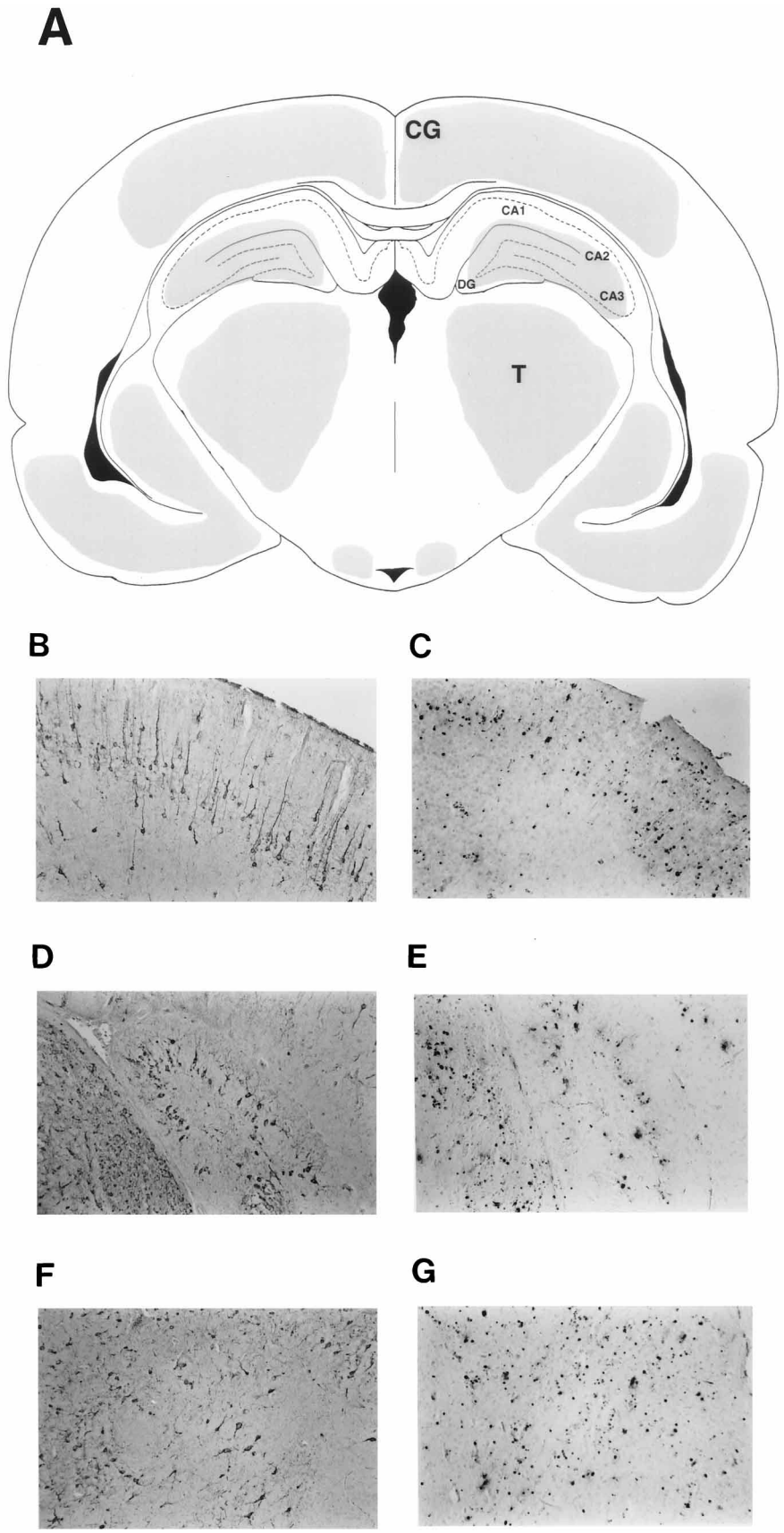

FIG. 2. (A) Schematic representation of a coronal section of mouse brain (modified from reference 21a, with permission from Academic Press), in which we have shaded areas of reovirus-infected and apoptotic cells, and tissue damage, 6 days after i.c. inoculation with T3D. Abbreviations: CG, cingulate gyrus; DG, dentate gyrus; and T, thalamus. (B to G) Reovirus antigen (B, D, and F)- and TUNEL (C, E, and G)-positive cells at 6 dpi within the cortex (B and C), the dentate gyrus (D and E), and the thalamus (F and G). Positive immunostaining for reovirus antigens appears as a dark precipitate in the cytoplasm, including neuronal processes. TUNEL-positive cells contain a dark precipitate in the nucleus. Original magnification, ×25.

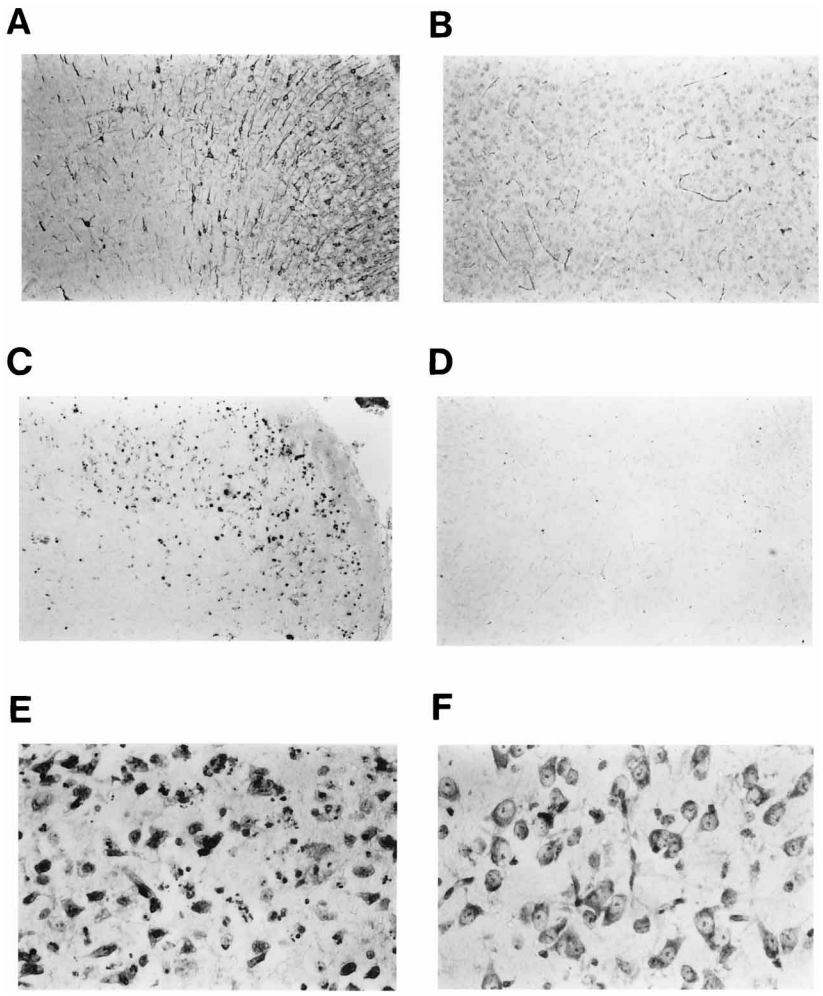

FIG. 3. Immunostaining for reovirus antigens in T3D (A)- and mock (B)-infected cingulate gyrus at 6 dpi; TUNEL assay on sections from T3D (C)- and mock (D)-infected cingulate gyrus at 6 dpi; cresyl violet staining of T3D (E)- and mock (F)-infected thalamus at 8 dpi. Original magnification for panels A to D, ×25; originial magnification for panels (E and F), ×100.

which has been eliminated by cell death due to reovirus infection. TUNEL-negative, reovirus antigen-positive cells may represent cells which are infected but have not yet become apoptotic or reached the stage of DNA fragmentation. Our observation that the number of reovirus antigen-positive cells appears to be significantly greater than the number of TUNEL-positive cells in some regions, like the hippocampus, suggests that cells may differ in their susceptibility to apoptosis. Neurons located in different regions of the brain may be more refractory to induction of apoptosis in general or by specific stimuli, due to variations in metabolic or developmental state or microenvironmental factors (7, 19).

Both direct and indirect mechanisms of apoptosis induction have been reported in studies of other viral infections. For example, HIV-induced apoptosis in lymph nodes appears to occur in uninfected bystander cells which are in close proximity to infected cells (4). Conversely, in Sindbis virus infection of mouse brain tissue the majority of apoptotic cells appear to be infected (13). Our findings suggest that tissue damage associated with reovirus infection results from induction of apoptosis by a combination of direct and indirect mechanisms. However, it is also possible that reovirus induces apoptosis of infected cells directly, but because of the putative difficulties in colabeling reovirus-infected, apoptotic cells and the unknown time frame between infection and detection of apoptosis, cells which are either reovirus antigen positive or TUNEL positive are detected more frequently than doubly labeled cells.

We have shown previously that reovirus induces apoptosis and inhibits host cell DNA synthesis in cultured fibroblasts (32, 33) and that strain-specific differences in both capacities are determined by the S1 gene, which encodes the viral attachment protein, σ1 (11, 37). UV-inactivated, replication-incompetent reovirus also induces apoptosis in cultured fibroblasts, suggesting strongly that early events in reovirus replication are sufficient for induction of apoptosis. However, the amount of input virus required is substantially greater than that required when replication-competent virus is used, suggesting that induction of apoptosis requires more virus than is required to initiate productive infection. Thus, completion of the replication cycle after infection initiated at low multiplicities of infection may be necessary only as a means of increasing the number of viral particles to a level sufficient for induction of apoptosis. Gaulton and Greene showed that inhibition of DNA synthesis in neuroblastoma cells could be mediated by an anti-reovirus type 3 receptor monoclonal antibody (5), a finding that supports the idea that σ1-mediated binding of reovirus to cell

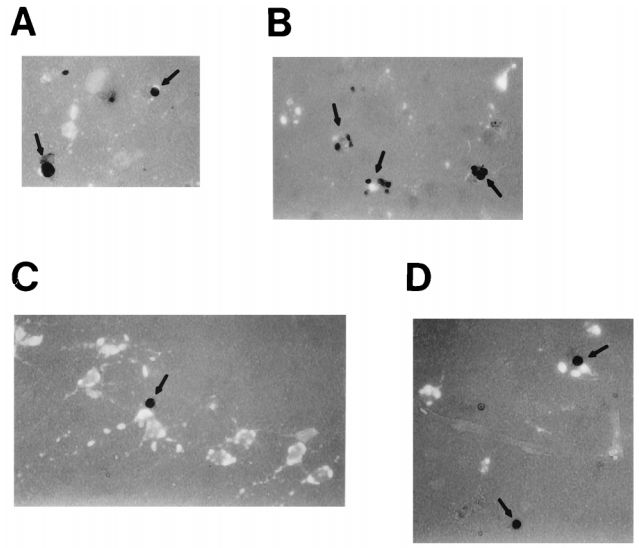

FIG. 4. Double-labeling assay for reovirus antigens (FITC) and TUNEL (dark precipitate) in T3D-infected sections. A double exposure under fluorescence and light microscopy allows detection of both reovirus antigen- and TUNEL-positive cells. (A) Cells within the cingulate gyrus, 8 dpi. Arrows show two cells which are colabeled for reovirus antigens and fragmented DNA (TUNEL). Antigen staining appears as a thin halo surrounding the dark, TUNEL-positive nucleus as a result of cytoplasmic shrinkage. (B) Cortical cells, 8 dpi. Arrows show cells which appear to be colabeled for reovirus antigens and fragmented DNA and have formed multiple apoptotic bodies. (C) Cells within the hippocampus, 6 dpi. Multiple neurons contain reovirus antigen but are TUNEL-negative. The arrow shows a TUNEL-positive nucleus adjacent to antigen-positive cytoplasm of a neuron. (D) Cells within the cingulate gyrus, 8 dpi. The upper arrow shows a TUNEL-positive nucleus adjacent to reovirus antigen-positive bodies. The lower arrow shows a TUNEL-positive nucleus in the absence of reovirus antigen staining. Original magnification, ×100.

surface receptors can have profound effects on the cell in the absence of viral replication. DNA synthesis inhibition mediated by the anti-idiotypic, antireceptor antibody required a critical threshold of signal resulting from either binding of a critical number of antibody molecules or the simultaneous engagement of multiple receptors. Binding of either the anti-idiotypic, antireceptor antibody or reovirus to receptors on R1.1 T lymphocytes was shown to activate receptor tyrosine kinase activity in addition to inhibiting cellular proliferation (26).

These in vitro findings suggest that the binding of reovirus to cell surface receptors via σ1 is sufficient for reovirus-mediated DNA synthesis inhibition and perhaps induction of apoptosis. They also suggest a mechanism for reovirus-induced apoptosis of uninfected, bystander cells in infected brain tissue in which large amounts of virus released from a productively infected cell induce apoptosis of neighboring cells as the result of the binding of a sufficiently large number of virus particles. In this model, apoptosis is induced in the presence of virus particles before productive infection occurs. Therefore, cells may be TUNEL-positive but the amount of viral antigen may be inadequate for detection by conventional immunohistochemical methods. A similar indirect mechanism has been suggested to occur during HIV infection, in which induction of apoptosis appears to occur primarily in uninfected, bystander cells in close proximity to infected cells. In this case, uninfected $CD4^+$ T cells with bound gp120 (from cell-to-cell contact with an infected cell) are killed via immune-mediated responses (4). A similar phenomenon, perhaps involving cytokines, could also explain the presence of uninfected, apoptotic cells neighboring reovirus-infected cells.

These observations suggest a model in which reovirus induction of apoptosis and DNA synthesis inhibition are mediated by a concentration-dependent binding of σ1 to cellular receptors, an event which may initiate or perturb transduction of signals from the cell surface to the nucleus, resulting in activation of the apoptotic pathway and/or inhibition of DNA synthesis. Although the relationship between these two phenomena in reovirus-infected cells is not yet understood, their common mechanism of induction suggests an overlap in subsequent events, the consequences of which may vary in dividing versus nondividing cells. Parallel signal transduction pathways and redundancy in signaling are not uncommon (3, 17, 34). The demonstration of reovirus-induced apoptosis of neurons in vivo, as shown in this report, indicates that inhibition of DNA synthesis is not required for apoptosis. It is interesting that the outcome of receptor tyrosine kinase signaling has been suggested to vary during development depending on small differences in ligand concentration which could lead to sustained versus transient activation (17). Reovirus, as a ligand, might also mediate different signaling responses depending on the concentration of virus particles bound to receptors during infection. Likewise, a dose-dependent induction of apoptosis versus necrosis has been shown for several compounds (12). In these cases, concentrations just below the necrosis-inducing threshold often resulted in induction of apoptosis instead. These observations suggest that induction of cell death is not simply a response to the presence of an inducer but is influenced by other factors such as concentration. In the case of virus infections, this might represent another mechanism by which viruses can avoid or delay cellular induction of apoptosis.

Virus-induced apoptosis has been postulated to represent a cellular response to infection that acts to curtail virus replication and spread by elimination of infected cells before completion of the viral life cycle. However, if virus replication is completed prior to induction of apoptosis, this putative defense mechanism is ineffective. Our data suggest that reovirus-induced apoptosis in infected mouse brain tissue does not affect viral replication but mediates significant tissue injury concurrently with maximal virus growth. The mechanism by which viruses induce and perhaps alter the course of the apoptotic response to infection is likely to vary with the virus and cell type and to involve a complex interplay among viral and cellular factors. Reovirus infection of cultured cells and neonatal mice provides a unique and well-defined model system for studying the mechanisms by which viruses induce apoptosis and the role of this process in viral pathogenesis.

ACKNOWLEDGMENTS

We thank J. John Cohen and Karen Sellins for many helpful discussions and critical review of the manuscript and Colin Kao for technical assistance.

This work was supported by a Merit Review Award from the Department of Veteran Affairs (K.L.T.), the core tissue culture and media facilities of the University of Colorado Cancer Center (K.L.T.), a virology-molecular biology training grant (NIH T32 NS0731) from the National Institutes of Health (K.L.T. and S.M.O.), a fellowship grant from the American Cancer Society and University of Colorado Cancer Center (S.M.O.), NIH grant NSO1741 (R.L.S.), Public Health Service Award AI32539 from the National Institute of Allergy and Infectious Diseases, and the Elizabeth B. Lamb Center for Pediatric Research (T.S.D.).

REFERENCES

1. **Auwaerter, P. G., H. Kaneshima, J. M. McCune, G. Wiegand, and D. E. Griffin.** 1996. Measles virus infection of thymic epithelium in the SCID-hu

mouse leads to thymocyte apoptosis. J. Virol. **70:**3734–3740.
2. **Clark, G.** 1981. Nissl staining with cresyl violet acetate, thionin, or toluidine blue O, p. 142. *In* G. Clark (ed.), Staining procedures, 4th ed. Williams and Wilkins, Baltimore, Md.
3. **Coughlin, S. R., J. A. Escobedo, and L. T. Williams.** 1989. Role of phosphatidylinositol kinase in PDGF receptor signal transduction. Science **243:**1191–1194.
4. **Finkel, T. H., G. Tudor-Williams, N. K. Banda, M. F. Cotton, T. Curiel, C. Monks, T. W. Baba, R. M. Ruprecht, and A. Kupfer.** 1995. Apoptosis occurs predominately in bystander cells and not in productively infected cells of HIV- and SIV-infected lymph nodes. Nat. Med. **1:**129–134.
5. **Gaulton, G. N., and M. I. Greene.** 1989. Inhibition of cellular DNA synthesis by reovirus occurs through a receptor-linked signaling pathway that is mimicked by antiidiotypic, antireceptor antibody. J. Exp. Med. **169:**197–211.
6. **Gavrieli, Y., Y. Sherman, and S. A. Ben-Sasson.** 1992. Identification of programmed cell death in situ via specific labeling of nuclear DNA fragmentation. J. Cell Biol. **119:**493–501.
7. **Heron, A., H. Pollard, F. Dessi, J. Moreau, F. Lasbennes, Y. Ben-Ari, and C. Charriaut-Marlangue.** 1993. Regional variability in DNA fragmentation after global ischemia evidenced by combined histological and gel electrophoresis observations in the rat brain. J. Neurochem. **61:**1973–1979.
8. **Hrdy, D. B., D. N. Duby, and B. N. Fields.** 1982. Molecular basis of reovirus neurovirulence: role of the M2 gene in avirulence. Proc. Natl. Acad. Sci. USA **79:**1298–1302.
9. **Johnson, E. M., Jr., and T. L. Deckwerth.** 1993. Molecular mechanisms of developmental neuronal death. Annu. Rev. Neurosci. **16:**31–46.
10. **Kerr, J. F. R., A. H. Wyllie, and A. R. Currie.** 1972. Apoptosis: a basic biological phenomenon with wide-ranging implications in tissue kinetics. Br. J. Cancer **26:**239–257.
11. **Lee, P. W. K., E. C. Hayes, and W. K. Joklik.** 1981. Protein sigma 1 is the reovirus cell attachment protein. Virology **108:**134–146.
12. **Lennon, S. V., S. J. Martin, and T. G. Cotter.** 1991. Dose-dependent induction of apoptosis in human tumor cell lines by widely diverging stimuli. Cell Prolif. **24:**203–214.
13. **Lewis, J., S. L. Wesselingh, D. E. Griffin, and J. M. Hardwick.** 1996. Alphavirus-induced apoptosis in mouse brains correlates with neurovirulence. J. Virol. **70:**1828–1835.
14. **Lucia-Jandris, P., J. W. Hooper, and B. N. Fields.** 1993. Reovirus M2 gene is associated with chromium release from mouse L cells. J. Virol. **67:**5339–5345.
15. **MacDonald, R. G., T. P. Martin, and J. A. Cidlowski.** 1980. Glucocorticoids stimulate protein degradation in lymphocytes: a possible mechanism of steroid-induced cell death. Endocrinology **107:**1512–1524.
16. **Majno, G., and I. Joris.** 1995. Apoptosis, oncosis, and necrosis. *An overview of cell death.* Am. J. Pathol. **146:**3–15.
17. **Marshall, C. J.** 1995. Specificity of receptor tyrosine kinase signaling: transient versus sustained extracellular signal-regulated kinase activation. Cell **80:**179–185.
18. **Mori, I., T. Komatsu, K. Takeuchi, K. Nakakuki, M. Sudo, and Y. Kimura.** 1995. *In vivo* induction of apoptosis by influenza virus. J. Gen. Virol. **76:**2869–2873.
19. **Mu, X., J. He, D. W. Anderson, J. Q. Trojanowski, and J. E. Springer.** 1996. Altered expression of *bcl-2* and *bax* mRNA in amyotrophic lateral sclerosis spinal cord motor neurons. Ann. Neurol. **40:**379–386.
20. **Nibert, M. L., and B. N. Fields.** 1992. A carboxy-terminal fragment of protein μ1/μ1C is present in infectious subvirion particles of mammalian reoviruses and is proposed to have a role in penetration. J. Virol. **66:**6408–6418.
21. **Oppenheim, R. W.** 1991. Cell death during development of the nervous system. Annu. Rev. Neurosci. **14:**453–501.

21a. **Paxinos, G., and C. Watson.** 1982. The rat brain in stereotaxic coordinates, plate 23. Academic Press, Inc., New York, N.Y.

22. **Pekosz, A., J. Phillips, D. Pleasure, D. Merry, and F. Gonzalez-Scarano.** 1996. Induction of apoptosis by La Crosse virus infection and role of neuronal differentiation and human *bcl-2* expression in its prevention. J. Virol. **70:**5329–5335.
23. **Petito, C. K., and B. Roberts.** 1995. Evidence of apoptotic cell death in HIV encephalitis. Am. J. Pathol. **146:**1121–1130.
24. **Razvi, E. S., and R. M. Welsh.** 1995. Apoptosis in viral infections. Adv. Virus Res. **45:**1–60.
25. **Rodgers, S. E., E. S. Barton, S. M. Oberhaus, B. Pike, C. A. Gibson, K. L. Tyler, and T. S. Dermody.** 1997. Reovirus-induced apoptosis of MDCK cells is not linked to viral yield and is blocked by Bcl-2. J. Virol. **71:**2540–2546.
26. **Saragovi, H. U., A. Bhandoola, M. M. Lemercier, G. K. Mohammad Akbar, and M. I. Greene.** 1995. A receptor that subserves reovirus binding can inhibit lymphocyte proliferation triggered by mitogenic signals. DNA Cell Biol. **14:**653–664.
27. **Schwartzman, R. A., and J. A. Cidlowski.** 1993. Apoptosis: the biochemistry and molecular biology of programmed cell death. Endocrine Rev. **14:**133–151.
28. **Shen, Y., and T. E. Shenk.** 1995. Viruses and apoptosis. Curr. Opin. Genet. Dev. **5:**105–111.
29. **Tsunoda, I., C. I. B. Kurtz, and R. S. Fujinami.** 1996. Apoptosis as a possible mechanism for elimination of virus infected cells from the central nervous system leading to demyelinating disease, p. 45. *In* Keystone Symposium, Cell Biology of Virus Entry, Replication and Pathogenesis. Keystone Symposia, Silverthorne, Colo.
30. **Tyler, K. L., R. T. Bronson, K. B. Byers, and B. N. Fields.** 1985. Molecular basis of viral neurotropisms: experimental reovirus infection. Neurology **35:**88–92.
31. **Tyler, K. L., and B. N. Fields.** 1996. Reoviruses, p. 1597–1624. *In* B. N. Fields, D. M. Knipe, P. M. Howley, et al. (ed.), Virology, 3rd ed. Raven Press, New York, N.Y.
32. **Tyler, K. L., M. K. T. Squier, A. L. Brown, B. Pike, D. Willis, S. M. Oberhaus, T. S. Dermody, and J. J. Cohen.** 1996. Linkage between reovirus-induced apoptosis and inhibition of cellular DNA synthesis: role of the S1 and M2 genes. J. Virol. **70:**7984–7991.
33. **Tyler, K. L., M. K. T. Squier, S. E. Rodgers, B. E. Schneider, S. M. Oberhaus, T. A. Grdina, J. J. Cohen, and T. S. Dermody.** 1995. Differences in the capacity of reovirus strains to induce apoptosis are determined by the viral attachment protein σ1. J. Virol. **69:**6972–6979.
34. **Valius, M., and A. Kazlauskas.** 1993. Phospholipase C-γ1 and phosphatidylinositol 3 kinase are the downstream mediators of the PDGF receptor's mitogenic signal. Cell **73:**321–334.
35. **Virgin, H. W., IV, R. Bassel-Duby, B. N. Fields, and K. L. Tyler.** 1988. Antibody protects against lethal infection with the neurally spreading reovirus type 3 (Dearing). J. Virol. **62:**4594–4604.
36. **Weiner, H. L., D. Drayna, D. R. Averill, and B. Fields.** 1977. Molecular basis of reovirus virulence: role of the S1 gene. Proc. Natl. Acad. Sci. USA **74:**5744–5748.
37. **Weiner, H. L., M. L. Powers, and B. N. Fields.** 1980. Absolute linkage of virulence and central nervous system tropism of reoviruses to viral hemagglutinin. J. Infect. Dis. **141:**609–616.